February 12, 2004

Int'l Bureau

FEB 17 2004

Front Office

Ms. Marlene H. Dortch
Secretary
Federal Communications Commission
445 12th Street, SW – Room TW-A325
Washington, D.C. 20554

Re: Call Sign E000723, File No. SES-MOD-20030512-00639

Dear Ms. Dortch:

In accordance with Special Condition 5948 of the above-referenced earth station license,[1] The Boeing Company ("Boeing") hereby submits the attached Boeing AMSS System License Compliance Report - Reflector Antenna Update. This updated report verifies that operation of Boeing's reflector antenna AES complies with all conditions and specific design guidelines set forth in paragraph 19(h)(1)-(5) of the associated AMSS licensing order.[2]

---

[1] *See* Radio Station Authorization, File No. SES-MOD-20030512-00639, Call Sign E000723 at 5. This condition requires Boeing to submit a report verifying its ability to comply with the conditions set forth in ¶19(h) of its AMSS licensing order no later than 30 days prior to commencing commercial operations with reflector antenna AESs. *See The Boeing Company*, Order and Authorization, 16 FCC Rcd 22645 (Int'l Bur./OET 2001) (*"Order"*).

[2] *See Order* at ¶19(h)(1)-(5).

If you have any questions concerning this submission, please contact the undersigned.

Respectfully submitted,

Philip L. Malet
Carlos Nalda
Steptoe & Johnson LLP
1330 Connecticut Avenue, N.W.
Washington, D.C. 20036
(202) 429-3000

Counsel for The Boeing Company

Attachment

cc (w/ att.):   Tom Tycz
                Howard Griboff
                Karl Kensinger
                Arthur Lechtman

Boeing AMSS System License Compliance Report --
Reflector Antenna AES Update

This Update to Boeing's prior License Compliance Report[1] is submitted pursuant to Special Condition 5948 of earth station authorization Call Sign E000723, and verifies that operation of Boeing's reflector antenna aircraft earth station (AES) with its licensed Aeronautical Mobile-Satellite Service (AMSS) system complies with the conditions of Boeing's AMSS licensing order and the specific design guidelines set forth in ordering clause ¶19(h)(1)-(5).[2] These design guidelines derive from work conducted in ITU-R working party 4A that was later incorporated into ITU-R Recommendation M.1643, and are designed to protect Fixed Satellite Service (FSS) operations from harmful interference from AES transmissions in the 14.0-14.5 GHz band.

Section 1 of this Update covers control and monitoring functions (¶19(h)(3)-(4)). Section 2 covers the control of aggregate off-axis EIRP (¶19(h)(1)). Section 3 covers factors that affect off-axis EIRP (¶19(h)(5.1)-(5.3)) including mis-pointing of AES antennas in Section 3.1, variations in AES antenna pattern in Section 3.2, and variations in AES transmit EIRP in Section 3.3. Resistance to being "pulled off" to adjacent satellites (¶19(h)(2)) is also covered in Section 3.1. The data presented in this Update shows that operation of Boeing's reflector antenna AES complies with significant margin to all conditions of the licensing order.

1 Control and Monitoring Functions

The addition of the reflector antenna to Boeing's AMSS system does not affect the control and monitoring functions that are included in the Boeing system to ensure that AES transmissions always remain under positive control, and to identify and shut down any malfunctioning AES, as described in Boeing's AMSS license application[3] and License Compliance Report.[4] The Boeing system will continue to be controlled by a network control and monitoring facility (NCMC) (¶19(h)(3)), which is referred to in this Update as the network operations center (NOC). The reflector antenna AESs will also continue to be

---

[1] *See* Boeing AMSS System License Compliance Report, File No. SES-LIC-20001204-02300, Call Sign E000723 (filed Aug. 14, 2002) ("Compliance Report").

[2] *See* Radio Station Authorization, File No. SES-MOD-20030512-00639, Call Sign E000723 at 5. This condition requires Boeing to submit a report verifying its ability to comply with the conditions set forth in ¶19(h) of its AMSS licensing order no later than 30 days prior to commencing commercial operations with its reflector antenna AESs. *See The Boeing Company*, Order and Authorization, 16 FCC Rcd 22645, File No. SES-LIC-20001204-02300, Call Sign E000723, DA 01-3008 (Int'l Bur./OET 2001) ("*Order*").

[3] *See Application of The Boeing Company for Blanket Authority to Operate up to Eight Hundred Technically-Identical Transmit and Receive Mobile Earth Stations Aboard Aircraft in the 11.7-12.2 and 14.0-14.5 GHz Frequency Bands*, File No. SES-LIC-20001204-02300 (December 4, 2000, supplemented January 10, 2001) ("Two-Way Application"), Technical Supplement at 5, 8-13, and 34-40.

[4] *See* Compliance Report at 1-3.

able to receive "enable transmit" and "disable transmit" commands (¶19(h)(4.1)), cease transmissions after receiving any "parameter change" command, which may cause harmful interference to other satellite systems during the change (¶19(h)(4.2)), continue to be monitored by the NOC to determine if its operation is malfunctioning (¶19(h)(4.3)), and will self-monitor and automatically cease transmissions in the event of an operation fault which can cause harmful interference to an adjacent FSS satellite (¶19(h)(4.4)).

2   Control of Off-Axis EIRP

The addition of the reflector antenna to the Boeing system does not fundamentally affect the algorithm employed by the NOC to control the aggregate off-axis EIRP of the system to less than or equal to that of a routinely processed very small aperture terminals (VSAT) terminal,[5] which is described in Boeing's license application[6] and License Compliance Report.[7]

The AES control algorithms used at the NOC accounts for variations in aggregate off-axis EIRP caused by, for example, mis-pointing of AES antennas, variations in AES antenna pattern from uncompensated radome effects, and variations in AES transmit EIRP (*see* Section 3). As described below, each element of the control algorithm is designed conservatively to compensate for each type of variation and ensure that the off-axis EIRP of Boeing's AESs remain within the levels prescribed for routinely processed VSAT terminals even in anticipated worst-case conditions.

The Boeing AMSS system control algorithm uses the reported state of all the AESs operating in the network and the known variations (tolerances and uncertainties) in the system to calculate the aggregate off-axis EIRP and control the individual AES transmissions, as described in Boeing's license application[8] and shown in Figure 1. All AES operating in the network report their position (latitude, longitude), attitude (heading, pitch, roll), and transmit EIRP[9] to the NOC. The NOC then uses the reported data, the known tolerances in AES pointing, antenna pattern, and transmit EIRP to compute an aggregate off-axis EIRP envelope for the AES operating in the network. This envelope is

---

[5] Loral Skynet, the operator of Telstar 6, has indicated to Boeing that it has coordinated Telstar 6 with the satellites adjacent to 93° W.L. for off-axis EIRP levels that are less than or equal to that of a routinely processed VSAT terminal. SES Americom, the operator of AMC-4, has also confirmed that it has coordinated AMC-4 with the satellites adjacent to 101° W.L. for similar off-axis EIRP levels.

[6] *See* Two-Way Application, Technical Supplement at 34-38.

[7] *See* Compliance Report at 3-5.

[8] *See* Two-Way Application, Technical Supplement at 34-38.

[9] *See* Boeing Two-Way AMSS Application, Technical Supplement at 37-38. The initial application indicated that the NOC would back-calculate the transmit EIRP of the AES based on the received power at the ground. Subsequent analysis has determined that it is more accurate for the AES to determine and report its EIRP to the NOC directly.

2

then compared to the off-axis EIRP limits for routinely processed VSAT terminals. Based on how closely the envelope approaches the limits, the NOC issues commands to allow additional AES into the network, change AES data rates/power levels, or remove AESs from the network.
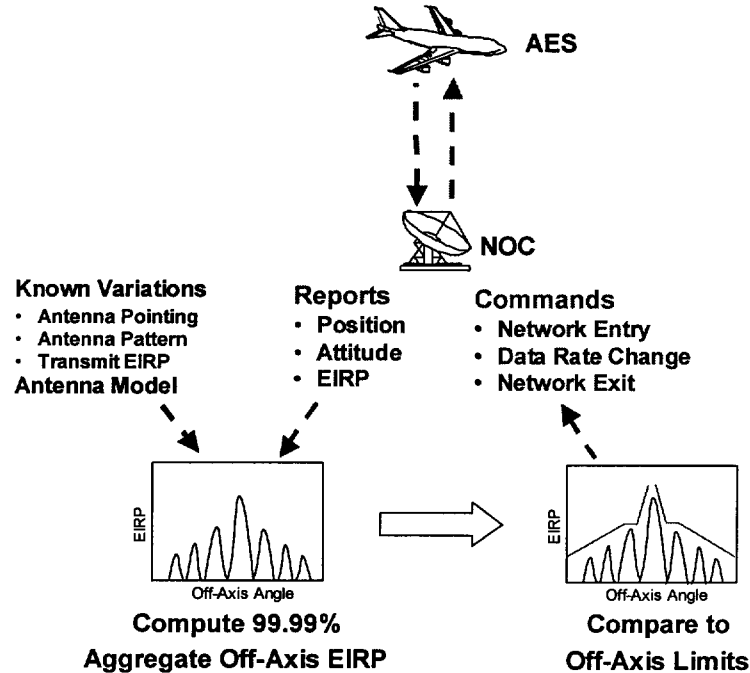

Figure 1. Control of Off-axis EIRP

An individual AES reports when its transmit EIRP, position or attitude (heading, pitch, roll) has changed sufficiently to cause its off-axis EIRP to change by more than 0.2 dB. The AES determines its position and attitude using information from the aircraft navigation data bus and concurrently calculates its EIRP based on the measured input power into the antenna and the measured antenna patterns.

Using the reported EIRP, the power spectral density (PSD) manager software at the NOC then calculates the antenna pattern gain envelope for each AES as projected along the GSO arc. The antenna model includes the antenna-pointing angles computed from the reported aircraft position and attitude. In comparison to the number of calculations needed to continuously calculate the phased array antenna pattern, generating an estimated gain pattern of the reflector antenna is greatly simplified. The phased array antenna pattern is a function of azimuth and elevation scan angles, polarization, frequency, and the temperature of each transmit module. Of these factors, the reflector antenna gain envelope is only a function of polarization and frequency due to the small affects of the radome as discussed in Section 3.2. Using the computed antenna gain envelope, the NOC then calculates the off-axis EIRP envelope for each AES by scaling the computed antenna pattern gain envelopes by the reported transmit EIRP.

3

A Monte Carlo method is used to combine the individual off-axis EIRP envelopes and the known factors affecting off-axis EIRP to calculate the aggregate off-axis EIRP envelope for the network. The Monte Carlo method allows combination of dissimilar factors that affect off-axis EIRP such as pointing tolerances (given in degrees) and power control tolerances (given in dB). The resulting envelope accounts for the 99.99% probability (or 3.7-sigma) combination of all of the tolerances and uncertainties in the system. This is equivalent to accounting for 3.7 times the root sum squared (RSS) of the 1-sigma affect on off-axis EIRP of each tolerance and uncertainty. Each of these factors are characterized in Section 3 (antenna mis-pointing, *see* Section 3.1, antenna pattern variation, *see* Section 3.2, and EIRP variation, *see* Section 3.3).

The calculated aggregate off-axis EIRP envelope is then compared to the limits for routinely processed VSAT systems. Boeing's AMSS system will not exceed the maximum co-polarized component along the GSO arc, which are as follows:

Angle off-axis	*Maximum EIRP in any 4 kHz band*
$1.0° \leq \theta \leq 7.0°$	$15 - 25 \log \theta$ dBW
$7.0° < \theta \leq 9.2°$	-6 dBW
$9.2° < \theta \leq 48°$	$18 - 25 \log \theta$ dBW
$\theta > 48°$	-24 dBW

The NOC recalculates the aggregate EIRP envelope whenever an AES makes a report and prior to admitting any AES to the network or permitting an AES to increase its data rate. The NOC controls AES data rate and entry into the system so that the aggregate off-axis EIRP limits are never exceeded.

3   Factors Affecting Off-Axis EIRP

Several factors may cause unintended variations in off-axis EIRP. These factors can be grouped into three categories: AES antenna mis-pointing, AES antenna pattern variation, and AES transmit EIRP variation. This section describes the testing that has been conducted which demonstrates that the Boeing system can and will adequately control these variations. The Boeing AMSS system has been designed to minimize each of these variations as well as to account for the effect of the variations in the control of the aggregate off-axis EIRP, as described in Section 2.[10] The major factor potentially affecting the reflector antenna off-axis EIRP is antenna mis-pointing. Antenna pattern variation and EIRP estimation are greatly simplified for the reflector antenna. As a result, control of the reflector antenna off-axis EIRP is less complex than for the phased array.

3.1   AES Antenna Mis-pointing

Several factors make the reflector antenna easier to point than the phased array antenna. For example, the use of one aperture for both transmit and receive eliminates the need to align two apertures. Also, the projected area of the reflector antenna does not vary

---

[10] *See Order* at ¶19(h)(5.1)-(5.3).

with pointing angle because the angular dimensions of the main beam does not vary with scan angle. These factors, as well as the demonstrated high performance of the antenna system rate gyros, improve pointing accuracy and reduce dependence on the reflector antenna sequential lobing function.

The reflector antenna system is designed to achieve a pointing accuracy of 0.25° 1-sigma in the azimuth plane (roughly along the GSO from mid-latitudes) and 0.6° 1-sigma in the elevation plane (roughly perpendicular to the GSO from mid-latitudes). These accuracies reflect RMS values over a time window of 100 sec in the presence of aircraft dynamics. The reflector antenna system will maintain this pointing accuracy in the maximum dynamic environment of a commercial aircraft. This is approximately 6°/sec in roll and 2°/sec in pitch and yaw/heading while airborne, and 10°/sec in heading on the ground. Transient errors due to very rapid transient dynamics may exceed the values above for short periods of time (e.g., 0.5 sec). If the reflector does exceed the budgeted control error, it automatically inhibits transmission.[11]

AES reflector antenna pointing is accomplished through a combination of high rate dynamic control to sense and compensate for airplane maneuvers, and periodic sequential lobing to refine estimates of static and slowly changing pointing bias parameters. Dynamic control uses data from the airplane navigation system and rate gyros mounted near the antenna to determine the motion of the antenna platform. The dynamic control function then commands the actuators to position the reflector to compensate for the platform motion (servo control), and hence keep the reflector boresight pointed to the satellite. The use of airplane navigation and rate gyro data and high rate control loop commands to the antenna (500 times per second) negate the need for the rapid sequential lobing used on the phased array. This high rate control provides the reflector antenna with an even greater ability to compensate for rapid AES motion than the phased array antenna.

The sequential lobing function measures and compensates for the net effect of a variety of possible pointing biases. This function is similar to the sequential lobing process used on the phased array antenna and uses the same received signal strength indicator (RSSI) measurement of forward link signal amplitude for estimating the true pointing direction to the satellite. Sources of pointing bias include changes of the alignment of the airplane navigation system to the antenna due to changing aircraft pressurization, fuel load, and flight state change; airplane navigation system attitude bias; RF squint compensation errors; and antenna azimuth and elevation axis bias errors. These pointing biases change gradually with time and antenna position. This gradual rate of change, along with the dynamic control function described above, allow for far less frequent sequential lobing cycles for the reflector antenna than for the phased array antenna. For the reflector AES, the sequential lobing frequency will be on the order of once every several minutes. Dynamic conditions such as changes in altitude, or antenna azimuth and elevation angles will cause more frequent sequential lobing to adjust for expected changes in pointing biases.

---

[11] As described in Boeing license application, the AES will still automatically inhibit when it loses the forward link. *See* Two-Way Application at 9.

Performance testing for dynamic control was conducted on both an antenna range 3-axis positioner and in-flight onboard a Boeing 737-400 test airplane. After initial integration and checkout on the 3-axis positioner, the 737-400 test bed was used to provide the most realistic environment for dynamic control performance testing. This test bed was equipped with a full suite of reflector AES equipment and control software. For these tests, antenna control was accomplished with operational control software, though special test software was used to provide very high rate data recording (500 samples / sec). Test flight conditions included level flight, high rate side to side rolls, and 90 deg heading changes.

Data from the high dynamics side to side roll (level to + 30° roll; to -20° roll, back to level) at roll rates of 6°/sec are shown in Figures 2 and 3. Figure 2 shows the dynamics of the roll maneuver, and Figure 3 shows the antenna server control error and the resulting total elevation and azimuth dynamic control error during the maneuver. Servo control performance, which measures the ability of the antenna control system to compensate for the measured motions of the airplane, was very good for this high rate maneuver. In addition to servo control performance, dynamic control performance includes the ability of the AES to determine the attitude of the antenna base in the presence of latencies in the airplane navigation data. To aid in latency compensation, the AES employs rate gyros mounted near the antenna. For dynamic performance evaluation, a 20 msec latency error in the navigation data was inserted into the post-processing. This latency represents one full data frame of the airplane navigation system roll and pitch data.
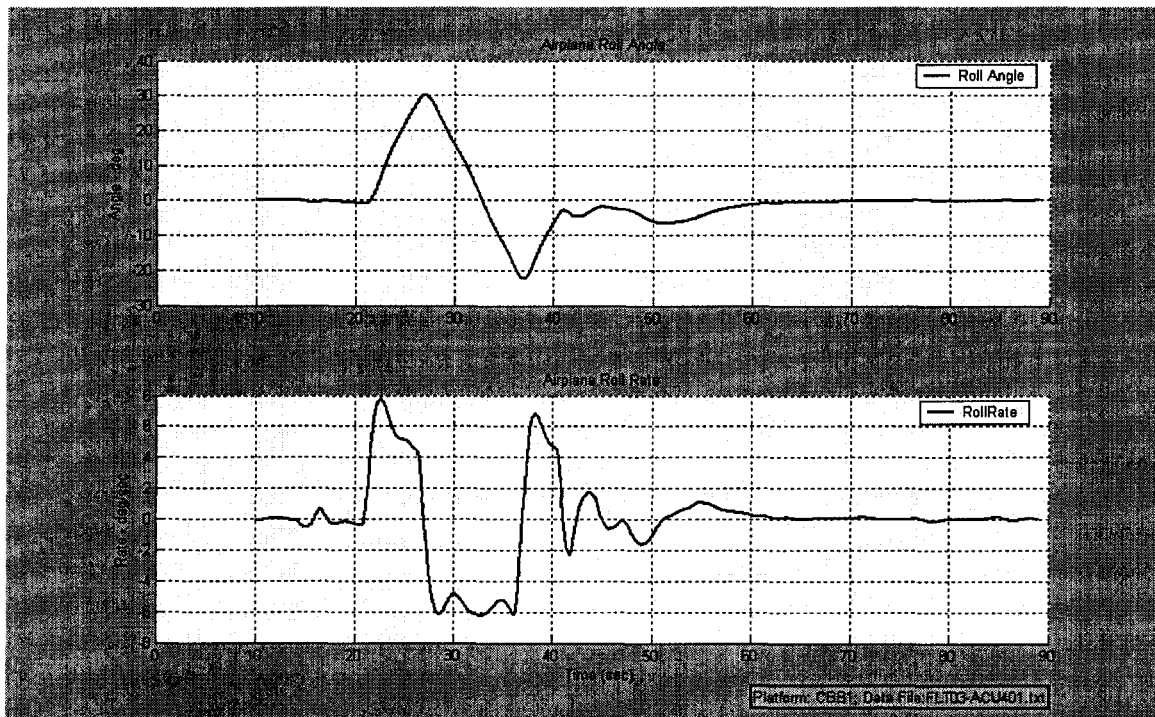

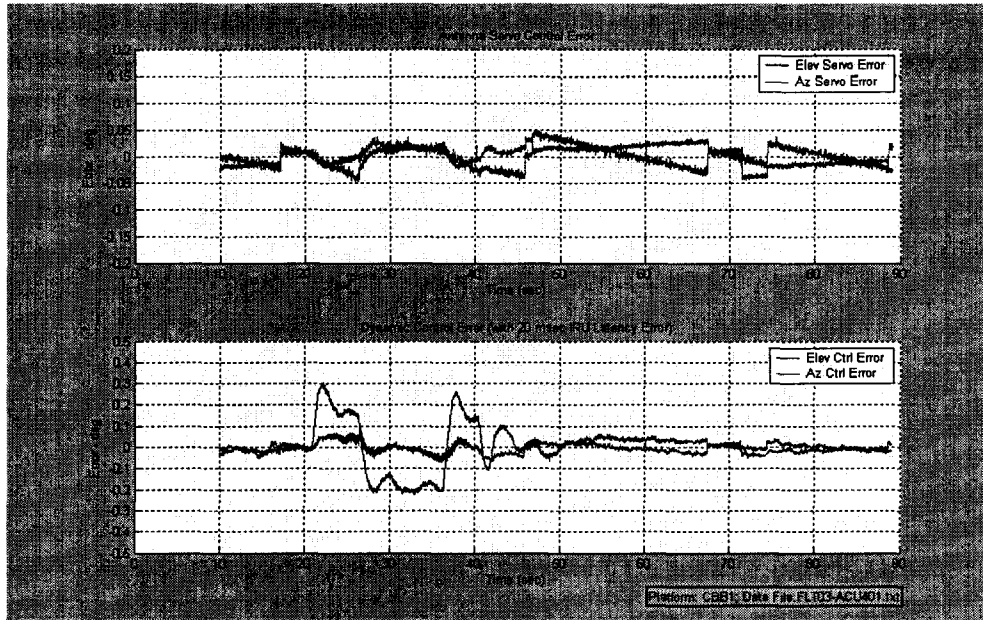**Figure 2: High Rate Side-to Side Roll: Airplane Maneuver**

Figure 3: High Rate Side-to Side Roll: Dynamic Control Performance

As mentioned above, the reflector antenna AES uses an RSSI sequential lobing process to refine its estimate of pointing bias errors. Previous testing of RSSI sequential lobing for the phased array antenna has shown this signal indicator to have no measurable susceptibility to being pulled off by adjacent satellite interference. AES pointing tests of the sequential lobing performance have been conducted in an indoor anechoic range, an outdoor range, and a fixed antenna site with a real satellite link, and onboard the Boeing 737-400 test bed aircraft. The indoor anechoic range provided the greatest flexibility for setting signal levels near lower thresholds, and for determining the reference truth model for performance assessment. The test setup on the indoor range is shown in Figure 4.

The truth references for the sequential lobing tests were established by measuring several hundred RSSI data points across the beam pattern, and then computing a polynomial curve fit to the collected data set. Sequential lobing was then exercised, and performance measured against the truth reference. Figures 5 and 6 show sample performance measurements for sequential lobing in the azimuth and elevation axes, respectively. The results of many independent tests of the sequential lobing function on the antenna range are shown in Figure 7.

Total reflector antenna AES pointing performance includes an allocation for change in pointing bias parameters between sequential lobing measurements, and uncertainties in receive beam to transmit beam radome squint (diffraction) compensation. The total per-axis root-mean-square (RMS) performance of the reflector antenna AES is computed as the root-sum-square (RSS) of these independent contributors (dynamic control, sequential lobing, changes between sequential lobing, and receive to transmit squint compensation uncertainty). These parameters combine to give an RMS pointing performance estimate of 0.24° in azimuth and 0.34° in elevation. These pointing

7

performance estimates fall below the initial allocations of 0.25° and 0.60° RMS for azimuth and elevation, respectively. The NOC uses these values when computing the aggregate off-axis EIRP envelope as described in Section 2.
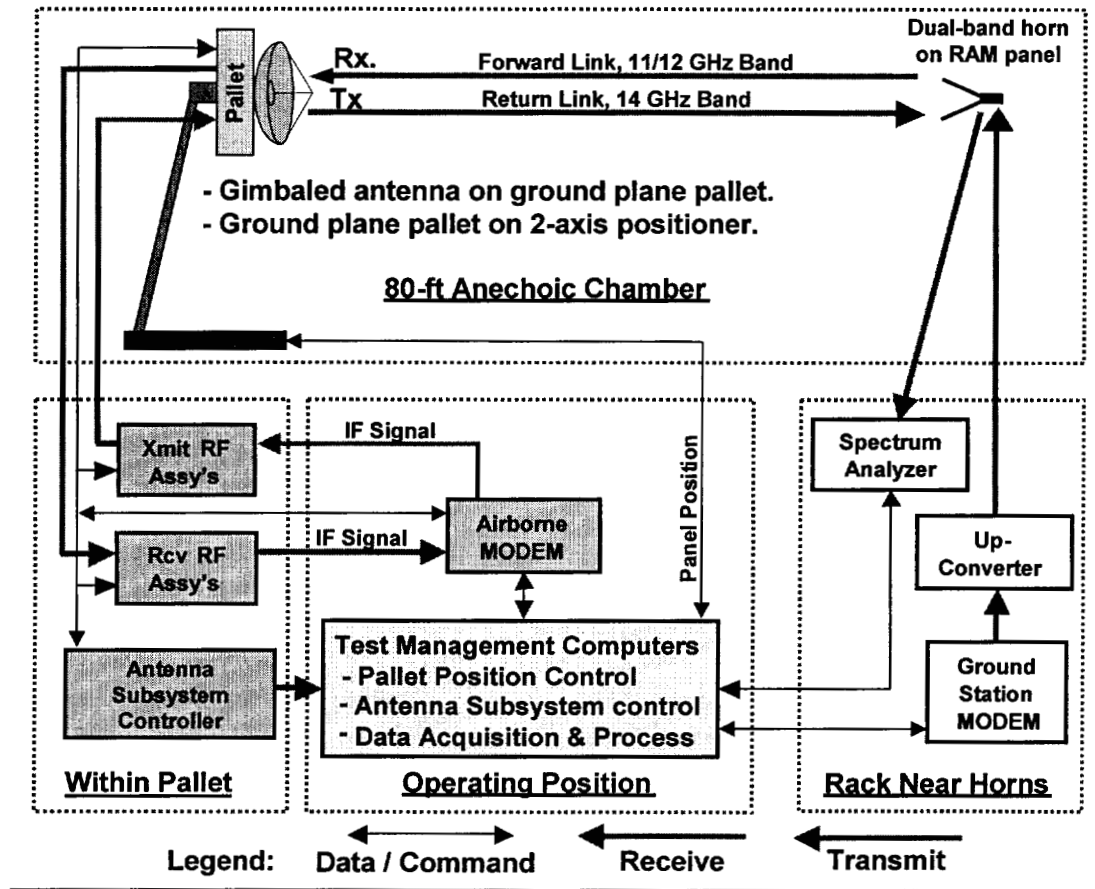

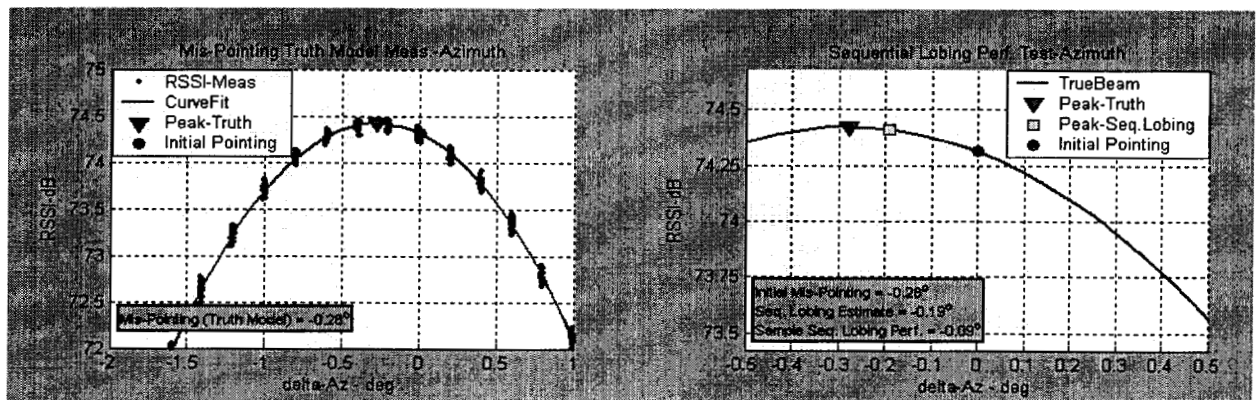**Figure 4: Test setup block diagram in indoor anechoic range**

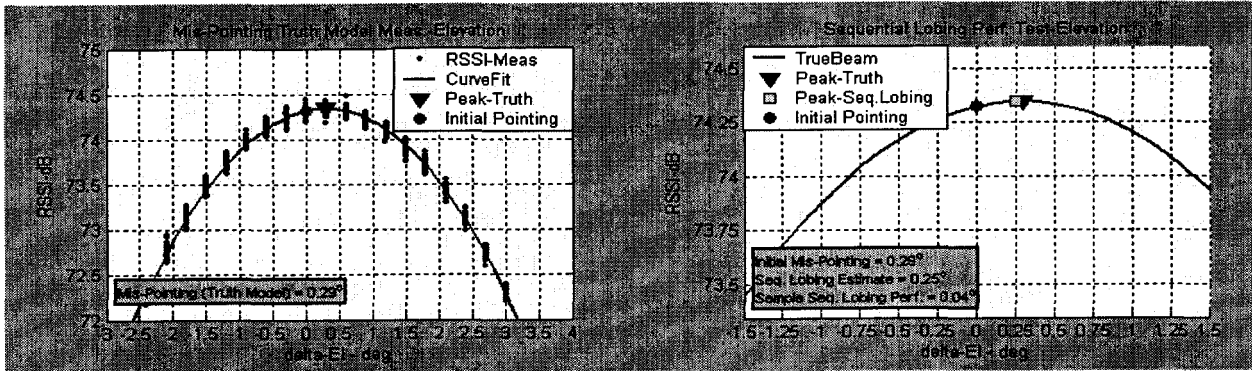**Figure 5: Sample Sequential Lobing Performance Measurement – Azimuth**

Figure 6: Sample Sequential Lobing Performance Measurement - Elevation
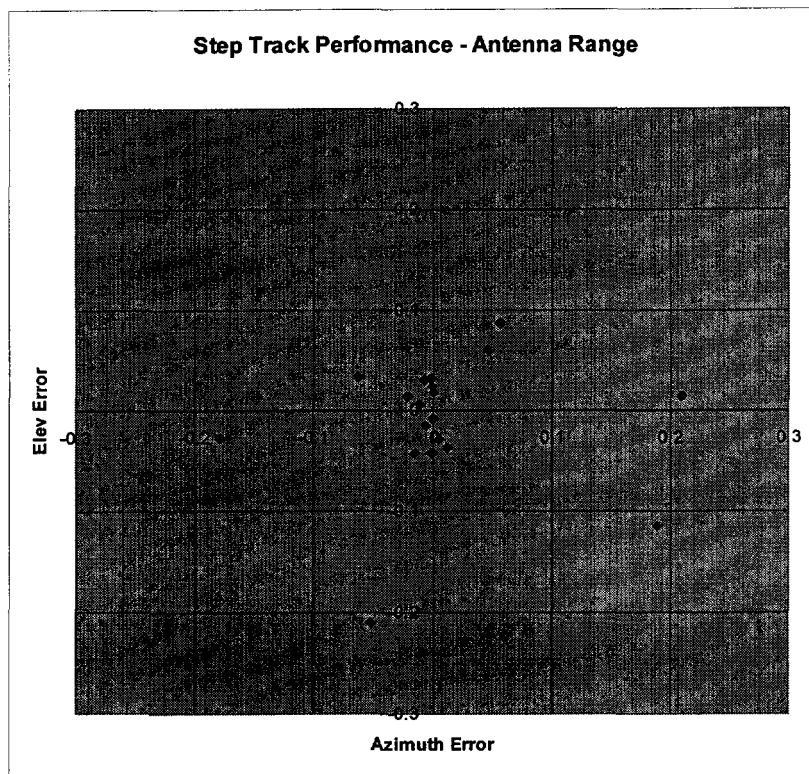

Figure 7: Step Track Performance

3.2 Antenna Pattern Variation

The antenna model used by the NOC will be substantially simplified with respect to the phased array antenna because the reflector antenna pattern varies little with antenna pointing angles (elevation and azimuth). In addition, reflector antennas have less unit-to-unit variation than phased array antennas. These two factors are the primary reason the reflector antenna patterns are generally easier to predict than the phased array antenna patterns. The antenna model used by the NOC will be based on the as-built performance of the reflector antenna, adjusted to account for unit-to-unit variation and radome effects.

The reflector antenna pattern data used by the NOC to calculate the contribution of a given airplane to the aggregate off-axis PSD levels along the GSO has been measured in a precision laboratory environment, with the antenna mounted for a "free-space" pattern measurement (*i.e.*, without the radome and without a simulated fuselage or any installation hardware). This approach provides pattern data which is independent of the antenna pointing direction, simplifying the PSD management software used by the NOC.

When installed on the airplane, the AES free-space antenna patterns will be perturbed by two effects: modification of the antenna patterns by the presence of the radome, and scattering and reflection from the airplane body (principally the region of the upper fuselage around the antenna) and from the installation hardware (principally the adaptor plate used to attach the antenna and radome to the airplane fuselage).

Extensive laboratory measurements have been made of the installed antenna patterns as a function of the antenna azimuth and elevation pointing angles, the antenna polarization angle and frequency. To simulate the impact of fuselage scattering and reflection on the antenna patterns, the antenna and radome were mounted to a truncated metallic cylinder of the same radius as a 737 airplane. The results show that the free-space antenna patterns are not significantly affected by either the presence of the radome or the simulated fuselage and antenna/radome adaptor plate. Figures 8 and 9 compare the installed and free-space azimuth and elevation patterns for a typical case. It is apparent that the installed patterns differ from the free-space patterns at relatively low pattern levels, but it has been shown that these pattern changes have little impact on the contribution to the aggregate off-axis PSD.
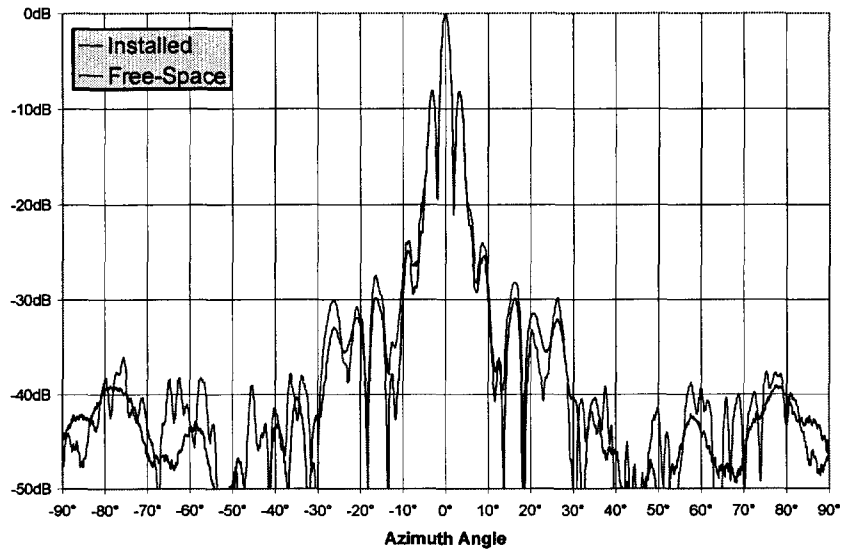
10

Figure 8: Measured Azimuth Antenna Patterns, Installed and Free-Space
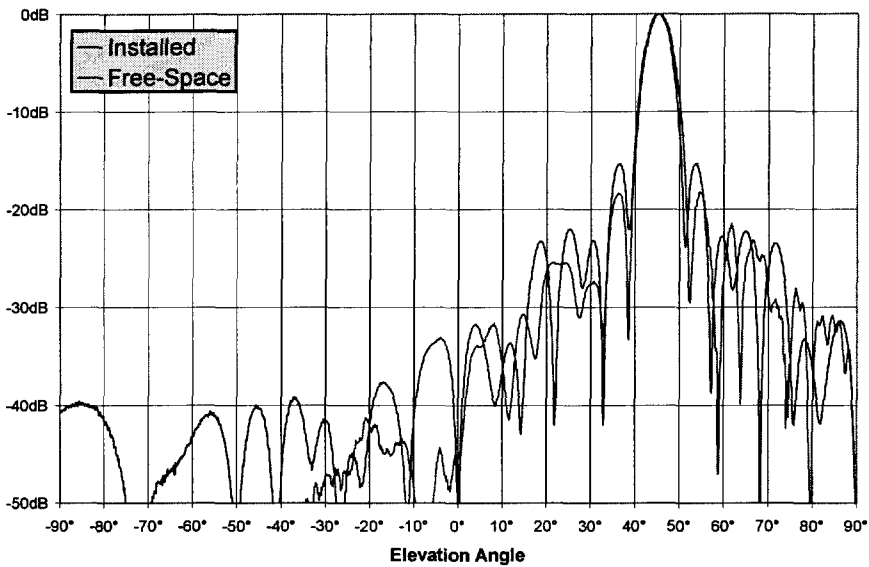

Figure 9: Measured Elevation Antenna Patterns, Installed and Free-Space

The measured free-space antenna pattern data used by the NOC to compute off-axis PSD levels along the GSO were measured for a single antenna. Any variation in pattern levels from antenna-to-antenna due to manufacturing tolerances (if at a significant level) would require that this variation be used in the off-axis PSD management budget. The antenna aperture is, however, an assembly of computer numerically controlled (CNC) machined components (main reflector and sub-reflector, sub-reflector support struts, and feed horn), with each part machined to stringent tolerances, and with the assembly

11

precisely aligned. On this basis it is expected that any antenna-to-antenna pattern variation will be minimal.

To confirm this, patterns were measured under closely identical conditions in the same antenna test range for two nominally identical antennas. Although the particular antenna design for these antennas was not identical to that of the production antennas, the differences were in only the detailed profiles of the two reflectors; in all other respects the design was identical to the production design, while the manufacturing and alignment processes were identical. Figures 10 and 11 compare measured transmit band patterns for the two nominally identical antennas in the azimuth and elevation planes respectively. It is apparent that any differences in the patterns are extremely small and essentially at the same level as differences between repeat measurements on the same antenna. For this reason there is no need to include antenna-to-antenna pattern variation as a contribution to the off-axis PSD management budget.
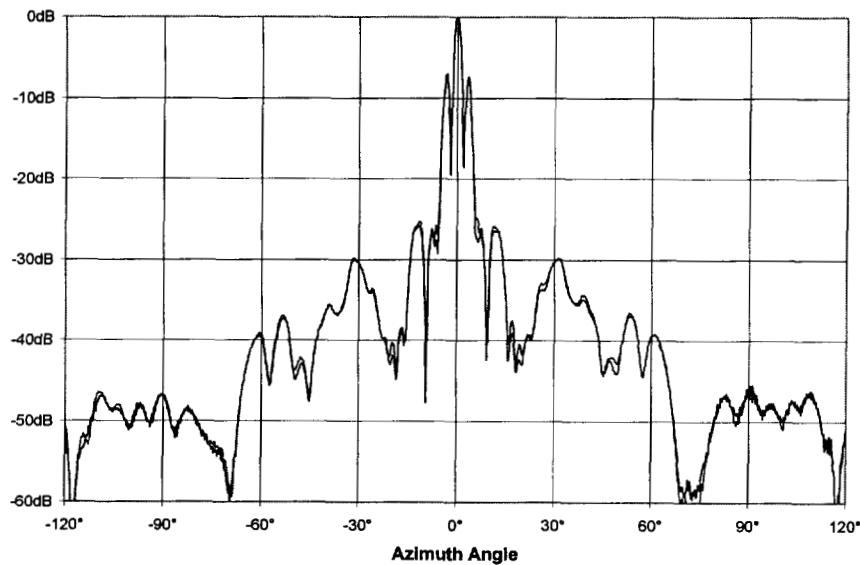

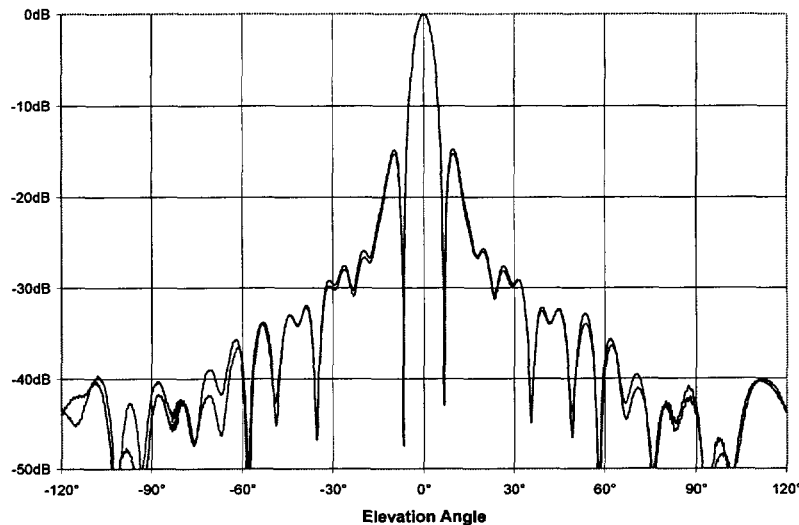**Figure 10: Measured Azimuth Pattern Comparison for Two Pre-Production Antennas**

Figure 11: Measured Elevation Pattern Comparison for Two Pre-Production Antennas

3.3 Transmit EIRP Variation

The transmit EIRP reported by reflector antenna AESs to the NOC will be more accurate than the EIRP reported by the phased array antenna because the input power to the reflector antenna is measured after output of the final high power amplifier and the reflector antenna gain is very predictable. Measuring the phased array transmit EIRP is more challenging because the input power is measured before the phased array elements, which act as a distributed high power amplifier, and because of the uncertainties in the electronic gain of the phased array. At maximum power, the reported EIRP uncertainty of the reflector antenna will be only 0.5 dB (1-sigma). This uncertainty includes radome effects on EIRP, frequency, polarization and pointing, and compares favorably to the reported EIRP uncertainty of 1.43 dB (1-sigma) of the phased array antenna. The NOC will account for this error when computing the off-axis EIRP envelope for the reflector antenna.

One component of the reported EIRP error budget is the error in reported EIRP under static conditions and with the radome removed. The value of EIRP reported by the AES under these conditions is determined by the AES by combining the measured value of SSPA output power with the known losses between the SSPAs and the antenna aperture and the know antenna directive gain. Both the SSPA/antenna losses and antenna gain is calibrated across the transmit frequency band. Additionally, the antenna gain is calibrated as a function of the transmit polarization angle. The SSPA output power is measured by calibrated power detectors located at the SSPA output ports. The detectors have been designed for high accuracy over the entire EIRP dynamic range, and are calibrated to remove the effects of sensitivity variation with both frequency and temperature.

The reported EIRP error has been measured in an antenna test range as a function of both commanded EIRP level and frequency. The true EIRP was determined for each point by measurement of the power received using a calibrated power meter from a calibrated standard gain horn located at the opposite end of the test range (at a known distance from the AES) as shown in Figure 4. The results of these measurements are

13

presented graphically in Figure 12. The peak reported EIRP error varies from 0.2 dB at the top end of the EIRP range to 0.6 dB at the lower end of the range, with typical values substantially lower. Based on these measurements the total EIRP estimation error used in the NOC will be 0.5 dB.
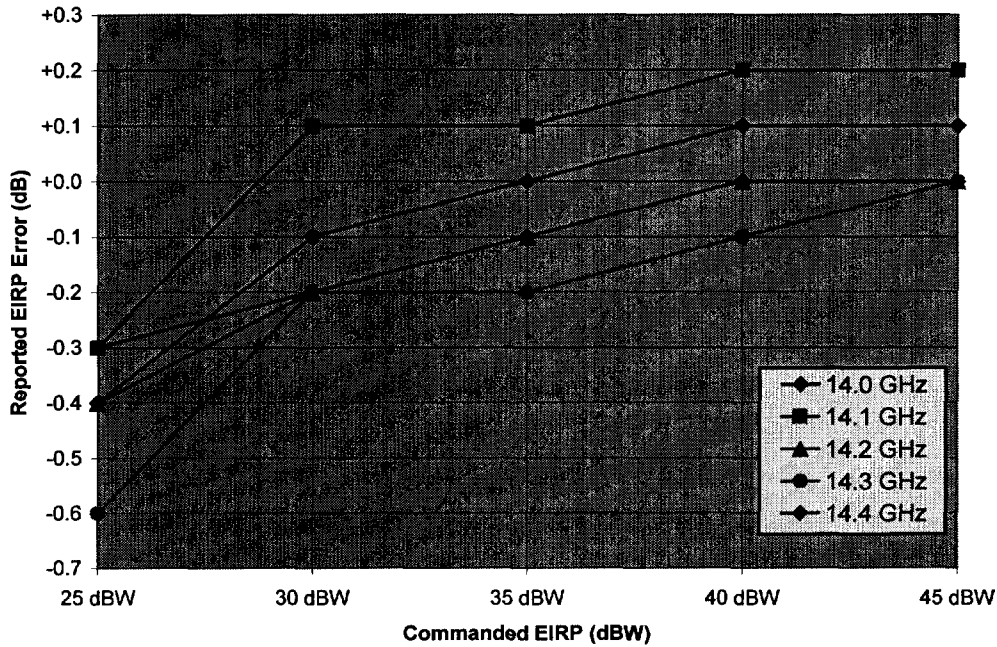

Figure 12: Measured Reported EIRP Errors (Static, No Radome)

3.4 Summary of Factors Affecting Off-Axis EIRP

The design, control, and testing of the reflector antenna AES for use with Boeing's AMSS system has addressed a wide variety of factors that affect the aggregate off-axis EIRP density of the system:

- Antenna mis-pointing (Section 3.1)
  - o Tracking error of closed loop tracking system
  - o Bias and latency of closed loop tracking system
  - o Pull-off to adjacent satellites
  - o Latency (of position and attitude inputs) and control error
- Antenna pattern variation (Section 3.2)
  - o Scanning angle variation (elevation and azimuth).
  - o Array pattern variation from radome
- Transmit EIRP variation (Section 3.3)
  - o Measurement error
  - o Cable loss calibration error

14

o   Unit-to-unit variation

By accounting for all of these factors, the Boeing AMSS system can control its off-axis EIRP density to within the limits for a routinely processed VSAT system.